PERGAMON

International Journal of Solids and Structures 37 (2000) 2495–2506

INTERNATIONAL JOURNAL OF SOLIDS and STRUCTURES

www.elsevier.com/locate/ijsolstr

Experimental and analytical evaluation of damage processes in thermal barrier coatings

S.Q. Nusier, G.M. Newaz*, Z.A. Chaudhury

Mechanical Engineering Department, Wayne State University, Detroit, MI 48202, USA

Received 20 September 1997; in revised form 5 November 1998

Abstract

Progressive damage evolution was evaluated using microscopy on samples subjected to a series of different thermal cycle profiles. Fick's law was used to describe the thermally grown oxide (TGO) buildup during early cycles. A correlation of damage thickness and oxide thickness for different thermal cycle profiles was established. The importance of this correlation is that, for a given thermal cycle profile and number of cycles, the oxide thickness can be calculated analytically using Fick's law, and from this thickness one can determine the interlayer separation (damage thickness). Both oxidation kinetics and interlayer separation (delamination) appear to have significant roles with respect to spallation. As early microcracks coalesce to form major delamination cracks or interlayer separation, the susceptibility for coating buckling is increased. The delamination cracks finally consume the TGO layer. Progressive microcrack linking is a possible mechanism to develop such critical delamination crack lengths. Physical evidence of buckling was found in specimens prior to complete spallation.

1. Introduction

Thermal barrier coatings (TBCs) provide thermal insulation and the bond coat supports a high temperature gradient at the surface of high temperature alloy substrates. Application of these superalloy/TBC systems can be found in both aerospace and land-based gas turbine engines. In automotive applications, the piston head for diesel engine is coated to achieve longer life time and higher performance in terms of fuel reduction and power. However, these coatings have durability problems, due to the material and thermal mismatch between the coating and the metallic substrate. Thermal residual stresses develop during cool down from processing temperatures (Nusier and Newaz, 1998; Chang et al., 1987; Williamson et al., 1993; Carapella et al., 1994; Evans et al., 1983).

* Corresponding author. Tel.: 001 313 577 3843; fax: 001 313 577 8789.
E-mail address: gnewaz@hub.eng.wayne.edu (G.M. Newaz)

0020-7683/00/$ - see front matter
PII: S0020-7683(98)00320-5

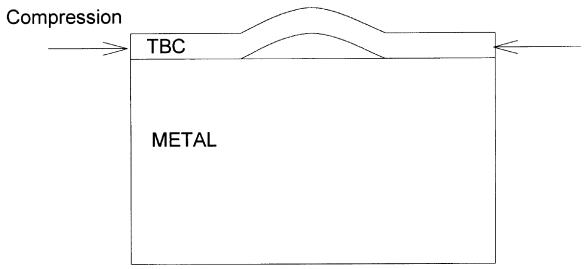

Fig. 1. Buckling-delamination model.

Environmental effects, specifically oxidation, and thermomechanical loading create additional stresses (Suo, 1995; Mikata and Taya, 1985; Kardomateas, 1989; Chung et al., 1985; Iwaki, 1986; Kardomateas, 1990; Kardomateas and Chung, 1994).

These stresses may initiate microcracks such as debonding and radial cracks and can have profound effects on the response of the TBC and interfacial damage accumulation and failure (Nusier and Newaz, 1998; Takeuchi and Kokini, 1994; Kokini and Hornack, 1988; Evans and Hutchinson, 1984; Bottega and Maewal, 1983a, b; Yin, 1985; Chai, 1990; Wan and Mai, 1995; Ryan and McCafferty, 1995). Their understanding is essential to predict the behavior of the coatings and their performance.

There are three most plausible scenarios that researchers have proposed to date to explain the spallation mechanism. Evans et al. (1983) proposed that due to cool down, planar compressive stresses within the TBC can lead to buckling, provided there is an interfacial delamination crack already present between the TBC and the substrate. They do not elaborate on how such a delamination crack may occur at the interface in the first place. Our recent calculations with the current EB-PVD TBC system show that the minimum delamination crack length required should be sixteen times the TBC thickness. Buckling of the TBC layer is illustrated in Fig. 1. We will term this failure model the Buckling Model. The growth of the delamination crack is possible due to local crack tip conditions which can experience both shear and out-of-plane tension. Another model for spallation is due to another author, Evans (1989). The basic aspect of this model is that through-thickness shear crack is developed in the TBC layer under compressive conditions in the TBC as shown in Fig. 2. This model can be termed the

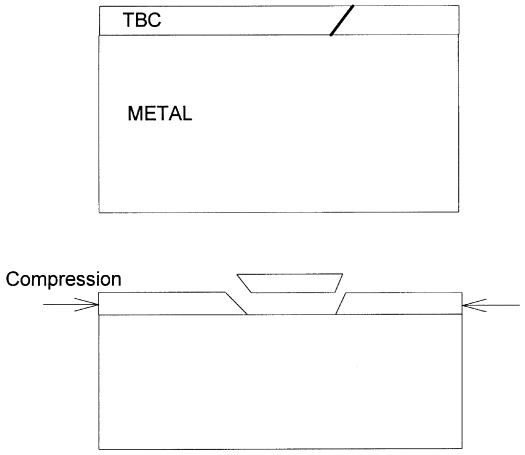

Fig. 2. Through-thickness shear model.

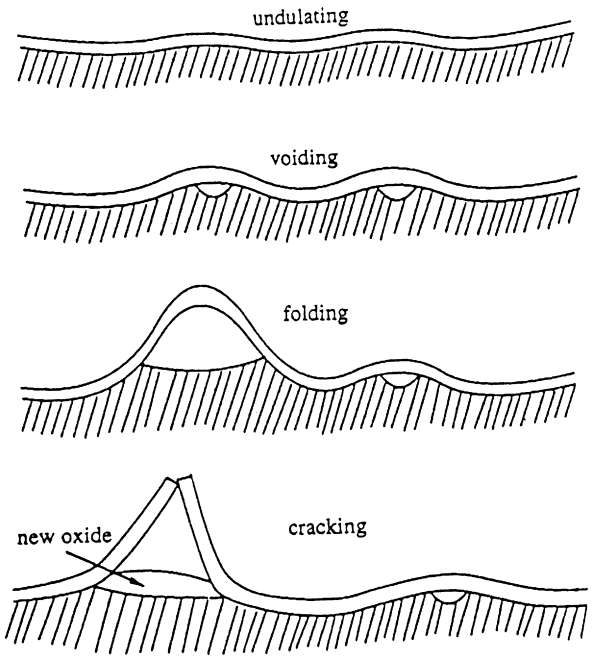

Fig. 3. Wrinkle model.

Through-Thickness Shear Model. Recently, Suo (1995) proposed the Wrinkle Model which was addressed earlier by a number of researchers (Siegler, 1993; Tolpygo and Grabke, 1994). According to this failure model, there is void formation under the TBC layer and folding effects may occur that lead to cracking of the TBC layer at various locations. The mechanism is illustrated in Fig. 3.

All of these models can be considered as *end-models* i.e. they describe the final spallation failure. However, the process of spallation is a gradual process as imposed thermal cycles continue to change the interfacial conditions and as oxidation and damage continue to evolve within the TGO layer leading to spallation at some critical stage. It is this evolution process that is the central theme of this work. The basic goal of our effort is to examine the nature of oxidation/damage evolution and attempt to describe the process mechanistically. Such information can be critical for developing mechanism-based life models by clearly identifying the underlying processes and to incorporate them into a realistic mechanics framework for life prediction.

2. Experimental aspects

The button specimens were 25.4 mm diameter by 3.17 mm thick button samples of nickel base superalloys Rene N5. There are two coats. The first one is the bond coat which is a diffusion aluminide PtAl alloy, which protects the alloy substrate from oxidation and bonds very well to both the alloy substrate and the outer EB-PVD thermally insulating TBC layer. The thickness of the bond coat is 0.0482 mm. The outer layer or the TBC is 8 wt% YSZ. The nominal thickness of the TBC layer is 0.127 mm.

The thermal cycle profiles used for conducting all tests for this research are shown in Fig. 4. Specimens were tested for various thermal cycles and examined after the thermal exposures. Specimens

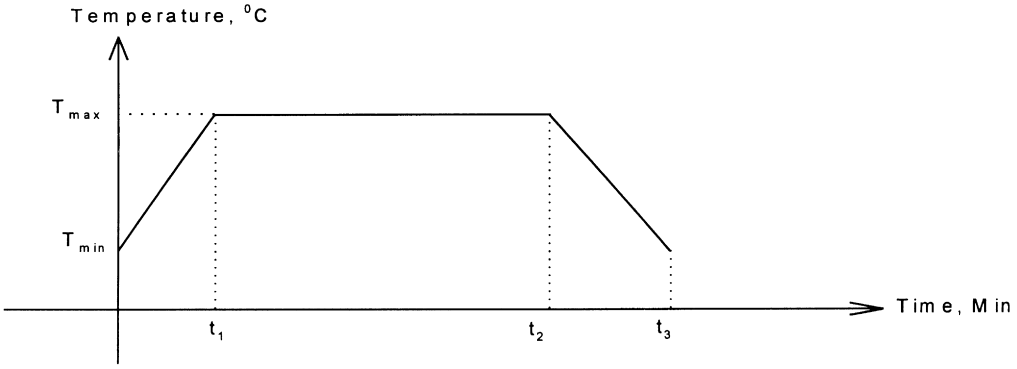

Cycle	T_{max}	T_{min}	t_1	t_2	t_3
A	1177	200	9	54	64
B	1132	200	9	54	64
C	1172	200	9	69	79
D	1172	200	9	609	619

Fig. 4. Thermal cycling profiles.

were evaluated at different numbers of thermal cycles. Complete spallation was observed in these specimens between 175–185 cycles (cycle A), 435–455 cycles (cycle B), and 100–205 cycles (cycle C). The thermally cycled samples were potted by using cold mounting epoxy resin. After curing for one day, the specimens were cut by using a Buheler Isomet 2000 diamond cutter. The samples were then ground and polished by using normal metallurgical procedures. The polished samples were observed under Olympus BX 60 optical microscope. A few samples were observed under a Hitachi 2000 Scanning Electron Microscope (SEM) at higher magnifications to observe the nature of delamination cracking within the TGO layer.

2.1. Thermal cycling

Thermal cycling tests on disk and cylindrical type samples were conducted on a rapid temperature CM furnace (model 1610 BL (c)). The heating zone for this furnace is about $20 \times 20 \times 25$ cm. To ensure the uniformity of the temperature, four different thermocouples (Type K) were used, two of them located at the bottom of the furnace and they are very close to the samples. The other two thermocouples were located at the top of the furnace. A digital recorder (Honeywell) was used to record the temperature variation. It should be mentioned that, the four thermocouples were showing a temperature difference of about 3–4°C at a temperature of 1177°C. A micristar controller was used to

set the parameters to define a thermal cycle, such as heat up time, hold time, cool down time, minimum temperature, and maximum temperature, etc.

3. Analytical aspects (growth of TGO layer)

The development of the diffusion model and the associated governing equations is necessary to determine the time dependent oxide layer thickness. Diffusion is approached as the penetration of one substance, such as oxygen, into a porous solid matrix of a different substance. Fick's second law can be used to model the diffusion of oxygen into the bond coat layer and subsequently the growth of the oxide layer (Neu and Sehitoglu, 1989a, b; Wittig, 1993; Aifantis, 1980; Wittig and Allen, 1994).

$$\frac{\partial c}{\partial t} = \left(Dc_{,i}\right)_{,i} \tag{1}$$

Eqn (1) is Fick's second law, where D is defined as the diffusion coefficient (μm^2/s), c is the oxygen concentration (atom/μm^3), and t denotes time dependence. The temperature dependence is incorporated into the diffusion coefficient which is approximated by an Arrhenius type relationship

$$D = D_0 \exp\left(\frac{-Q}{RT}\right) \tag{2}$$

where D_0 is the diffusion constant (μm^2/s), Q is the activation energy for oxygen diffusing into metallic substrate (J/mol), R is the universal gas constant (8.134 J/mol K) and T is the temperature (K). Neumann boundary conditions are incorporated along the free surface of the composite

$$D\frac{\partial c}{\partial x} + \alpha_S(C_S - C_O) = 0 \tag{3}$$

where α_s is a solubility coefficient related to the coating on the surface of the composite, C_S is the surface concentration, and C_O is the concentration of the outside medium.

The oxidation growth law will be obtained from the experiments as function of D_p^{eff} and time, where D_p^{eff} is the effective oxidation constant and is defined as

$$D_p^{\text{eff}} = \frac{1}{t_c}\int_0^{t_c} D_0 \exp\left(\frac{-Q}{RT(t)}\right)\mathrm{d}t \tag{4}$$

where $T(t)$ is the temperature which can vary with time.

The solution of the partial differential eqn (1) for a one-dimensional problem is obtained by using separation of variables technique in the following form

$$c(x, t) = C_O + (C_i - C_O)\sum_{n=0}^{\infty} B_n \cos\lambda_n(x/L)\mathrm{e}^{-\lambda_n^2 tD/L^2} \tag{5}$$

where,

$$B_n = \frac{4\sin\lambda_n}{2\lambda_n + \sin 2\lambda_n} \tag{6}$$

The eigenvalues λ_n are the roots for the following equation

$$\lambda_n \tan \lambda_n - \alpha_S L/D = 0 \tag{7}$$

The constants used for analysis in this investigation were as follows (Wright, 1996): activation energy for oxygen diffusion: $Q = 321$ kJ/mol; diffusion constant: $D_0 = 3.85 \times 10^{-5}$ m^2/s; universal gas constant: $R = 8.314$ J/mol K.

Let $q = \alpha_s L/D$, for the case where q is a large number. Eqn (7) can be solved in close form as follows, assume that the eigenvalues λ_n has the following form

$$\lambda_n = (2n-1)\frac{\pi}{2} - \varepsilon \tag{8}$$

where ε is a small number. By substituting eqn (8) into eqn (7) and expanding the tan in power series of ε, then solving for ε one can get

$$\varepsilon = \frac{(2n-1)\frac{\pi}{2}}{1+q} \tag{9}$$

Substituting eqn (9) into eqn (8) one gets

$$\lambda_n = (2n-1)\frac{\pi}{2}\left(\frac{q}{q+1}\right) \tag{10}$$

Bond coat oxidation resistance has been clearly linked to increased durability of the TBC. True properties of bond coats for analysis are difficult to obtain. Brindley (1995) has studied properties of plasma sprayed bond coats thoroughly which shed light on a number of properties of bond coats that may influence TBC life.

4. Results and discussion

The formation of an oxide layer can be easily traced via microscopy at the interface between the TBC layer and the bond coat as shown in Figs. 5–8. Fig. 5 shows the photomicrograph of a thermal barrier

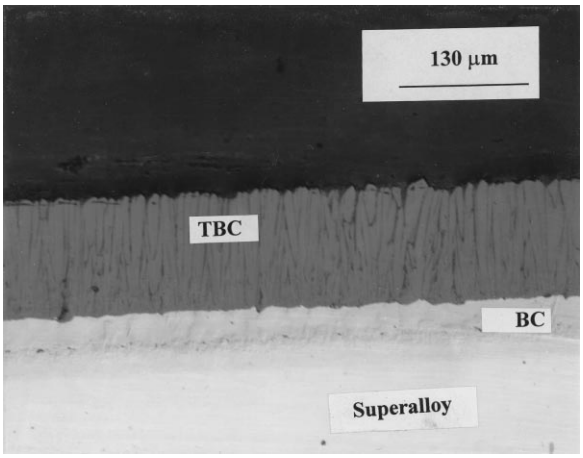

Fig. 5. An optical micrograph of an untested thermal barrier coated sample. Thermally grown oxide (TGO) layer and/or interfacial separation were absent at the bond coat/top coat (TBC) interface.

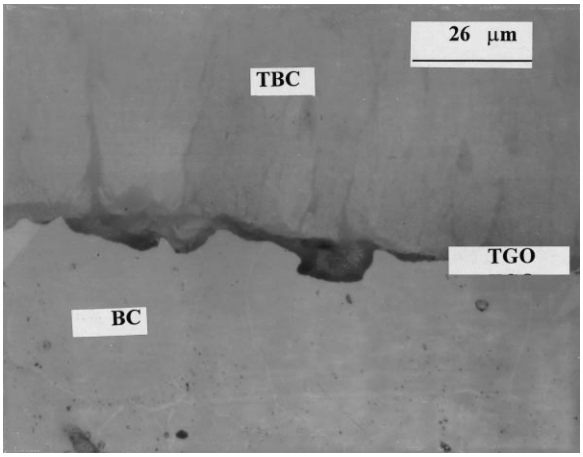

Fig. 6. An optical micrograph of a tested thermal barrier coated sample. Thermally grown oxide (TGO) layer and/or interfacial separation were seen at the bond coat/top coat (TBC) interface. The sample was thermally cycled to 25 cycle (type A).

coated sample without any thermal cycling. As expected, no interfacial cracking and thermally grown oxide layer were evident at the bond coat/top coat (TBC) interface. Thermal cycling of samples in air leads to the formation of a reaction product layer and interfacial cracking/damage at the bond coat/top coat interface. This oxidation product (TGO) is Al_2O_3 and has been confirmed by many researchers (Brindley, 1995). The TGO appears to grow thicker with a higher number of thermal cycles. Also, within the TGO layer, numerous microcracks and void like discontinuities are formed. A few thermal cycles leads to the formation of interfacial cracking at the bond coat/top coat interface and with an increasing the number of cycles leads to the formation of both interfacial cracking and TGO layer. Figs. 6 and 7 show the photomicrographs of the interfacial cracking at the bond coat/top coat interface taken after 25 and 50 thermal cycles (cycle type A). Fig. 8 shows the chronological evaluation of interfacial damage in TBC due to thermal cycling at 75 (cycle type A). The thickness of the TGO layer grows with increasing the number of cycles.

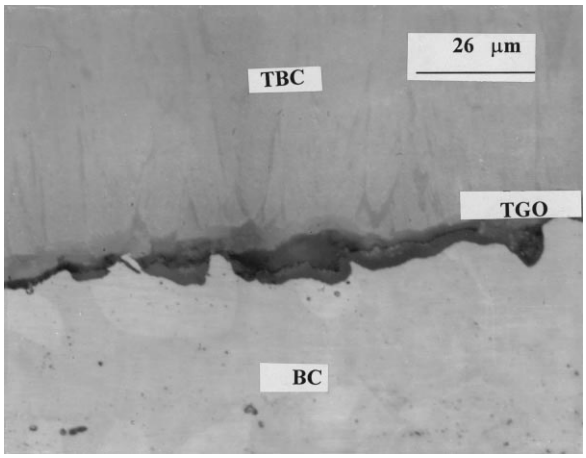

Fig. 7. An optical micrograph of a tested thermal barrier coated sample. Thermally grown oxide (TGO) layer and/or interfacial separation were seen at the bond coat/top coat (TBC) interface. The sample was thermally cycled to 50 cycle (type A).

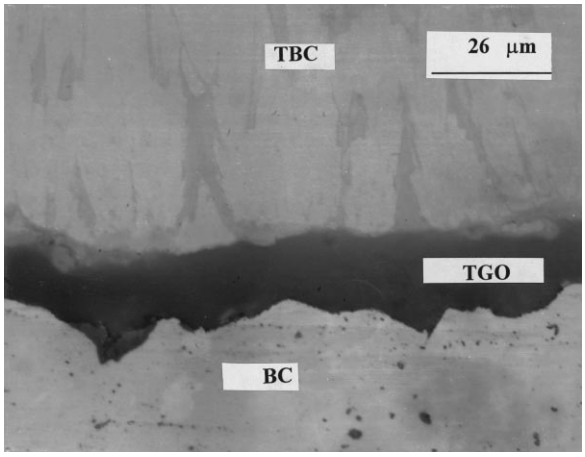

Fig. 8. An optical micrograph of a tested thermal barrier coated sample. Thermally grown oxide (TGO) layer and/or interfacial separation were seen at the bond coat/top coat (TBC) interface. The sample was thermally cycled to 75 cycle (type A).

After about 50 cycles (cycle type A), the TGO shows separation in the form of delamination. The separation between the TBC and the bond coat takes place through the TGO layer instead of delamination at any preferred interface. The TGO layer growth in addition to separation thickness is termed as 'damage thickness'. The damage thickness (Figs. 6–8) between the TBC and the bond coat continues to increase as the number of cycles is increased. We can address this cycle induced change by accounting for damage coalescence within the TGO layer and increased propensity for buckling of the TBC layer. We address this mechanism next.

Based on our analysis of top layer buckling on a circular plate, our estimates show that buckling is

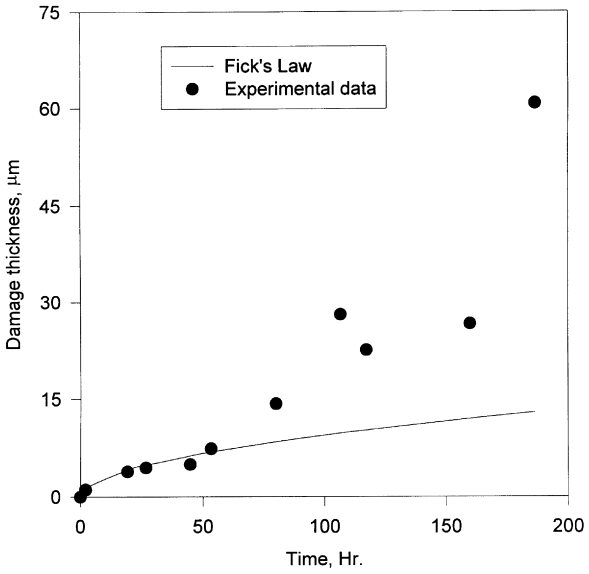

Fig. 9. Comparison of experimental data and prediction using Fick's law for TGO buildup as a function of the total cycle time for thermal cycle A.

possible only if the delamination crack size is 12–16 times or more the TBC thickness (Nusier and Newaz, 1998). The evidence of buckling in a specimen cycled to 175 (cycle type A) cycles, where the separation width for delamination is considerably higher at the middle of the specimen than near the ends, points out that the delamination crack through the TGO layer may reach such a critical length necessary to induce buckling. The evolution of damage in the form of microcracks and voids within this layer can interact to form such delamination cracks (Newaz et al., 1998).

For oxidation only driven degradation, the TGO layer growth can be described by Fick's law. The predicted TGO layer growth is shown in Fig. 9 for cycle A. Damage thickness in this study refers to any change in specimen structure. These changes can be oxide, separation, crack, voids, etc. Based on that, when we have breakdown of the TGO layer, we refer to the difference between damage thickness and oxide thickness as separation. The experimental data which is an average of at least four optical micrographs for each point along the length of the TGO layer is shown in the same Figure. A computer code (written in C^{++}) was developed to evaluate the damage area from which the damage thickness can be evaluated. The input for this program is the output of a scanned optical micrograph in TIF format.

The deviation of experimental results from the predicted TGO layer thickness occurs at about 50 thermal cycles (cycle A) and at 130 thermal cycles (cycle B). According to Fick's law, these two cycles have approximately the same oxide thickness. The significance of this result is that below 50 thermal cycles of the type chosen in this investigation, the TGO layer growth is oxidation driven.

According to eqn (4), for any thermal cycle profile, an effective diffusion constant can be evaluated by numerical integration. Simpson's rule was used. After the effective diffusion constant has been determined, the oxidation thickness according to eqn (5) can be evaluated. A very interesting result was found, i.e. the damage thickness (experimental measurement) is equal to the oxide thickness (Fick's law) up to a critical oxide thickness ($\cong 6.2$ μm). Beyond this thickness, the damage thickness starts to get bigger than the oxide thickness (separation thickness is the difference between damage thickness and oxide thickness). In other words, interfacial separation starts to take place. At another critical oxide thickness ($\cong 13$ μm) the samples spall off. This observation has been proven for different thermal cycle profiles; different maximum temperature and different holding times were used (cycles type A, B, C and

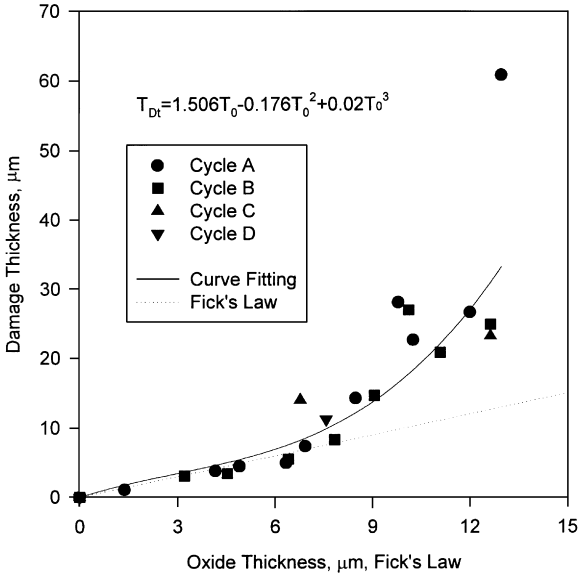

Fig. 10. Total damage thickness (experimental output) vs oxide thickness (Fick's law) for different thermal cycling profiles.

D). Fig. 10 shows the variation in total damage thickness versus oxide thickness for four different thermal cycles. This figure clearly shows that four different thermal cycle profile follow same trend to failure. An important outcome from this figure, is that, for any thermal cycle profile and at any time during thermal exposure, the oxide thickness can be calculated easily and straight forwardly by the use of Fick's law, knowing that the oxide thickness will lead to identifying the damage state (Fig. 10). To develop Fig. 10, the maximum temperature varied between 1177 and 1132°C (this is the recommended application temperature range for this kind of sample by GE) and the holding times varied between 45 and 600 min. As will be discussed later on, the holding time has no effect on damage size as long as the sum of holding time is fixed.

The maximum temperature has a major effect on life time, for example, reducing the maximum temperature from 1177°C to 1135°C will increase the sample life time by a factor of 2.4. This observation is illustrated in Fig. 11, which has been based on Fick's law and the critical oxide thickness to failure which is 13 μm. It is very clear that time to failure is highly dependent on the maximum temperature. A very important result that is obtained from this research is that the oxide thickness evaluated by Fick's law, can still be used as a correlation parameter to define the state of damage for any thermal cycle profile and at any time during thermal exposure.

Effect of holding time on damage accumulation was determined by running four samples under two different thermal cycle profiles (C and D). Two samples were run under each thermal cycle to make sure that the results were not influenced by any initial damage due to coating process. The sum of the

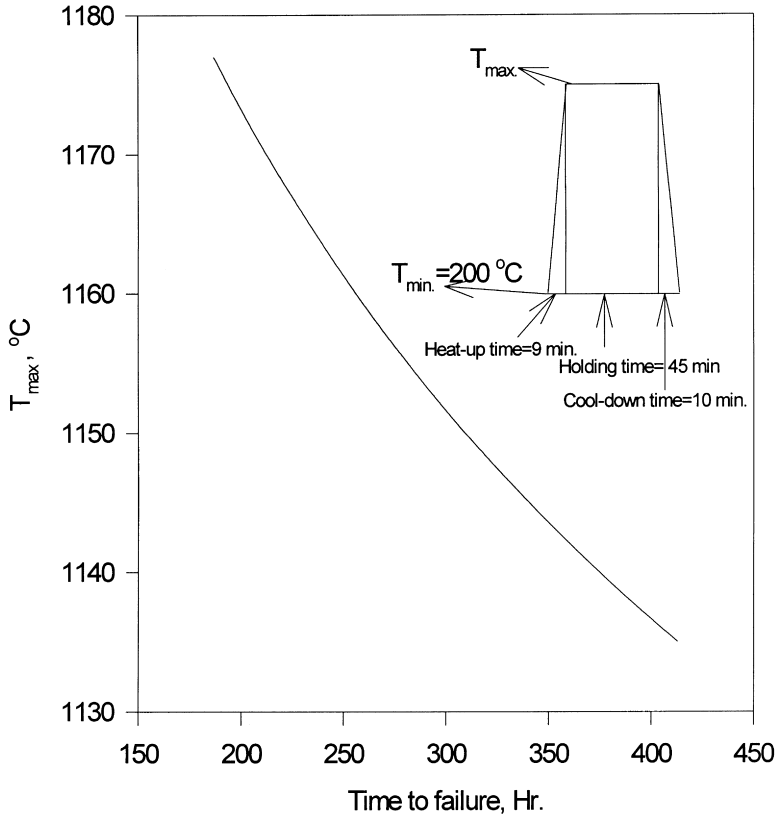

Fig. 11. Variation of T_{max} vs time to failure based on Fick's law and critical oxide thickness (13 μm).

holding time was fixed to a 50 h value. Finally, those samples were cut and observed under an optical microscope, the damage was almost identical.

Data for different thermal profiles can be grouped to establish a trend as shown in Fig. 10. Furthermore, a correlation between TGO thickness and damage thickness was obtained.

5. Summary and conclusions

Based on this investigation the following conclusions can be drawn:

1. Fick's law was used to describe the thermally grown oxide (TGO) buildup for early cycles. It was found that Fick's law can be used to correlate between damage thickness and oxide thickness for different thermal cycle profiles. The importance of this correlation is that, for a given thermal cycle profile and number of cycle, the oxide thickness can be found analytically using Fick's law, from this thickness one can determine the state of damage (damage thickness) by using the correlation formula.
2. The maximum temperature has a major effect on lifetime, for example, reducing the maximum temperature from 1177 to 1135°C will increase the sample lifetime by a factor of 2.4.
3. If the sum of the holding times is kept constant for the thermal cycle profiles considered, then it leads to similar damage state, i.e. isothermal and thermal cycling have similar damage states provided that the peak temperature is the same.
4. A major delamination crack can form at the TGO/bond coat interface. For large delamination cracks, in-plane compressive stress in the TBC layer due to the cool-down part of the thermal cycle can lead to spallation of the TBC layer due to buckling (Newaz et al., 1998).

Acknowledgements

Funding for this research was provided through a grant (No. F49620-95-1-0201) from the Air Force Office of Scientific Research (AFOSR). Dr Ozden Ochoa is the program monitor. Discussion and interaction with Dr P.K. Wright of GEAE is gratefully acknowledged.

References

Aifantis, E.C., 1980. On the problem of diffusion in solids. Acta Mechanica 37, 265–296.

Bottega, W.J., Maewal, A., 1983. Delamination buckling and growth in laminates. Transactions of the ASME 50, 184–189.

Bottega, W.J., Maewal, A., 1983. Dynamics of delamination buckling. International Journal of Non-Linear Mechanics 18 (6), 449–463.

Brindley, W.J., 1995. In: Properties of plasma sprayed bond coats. Proceedings of TBC Workshop. NASA-LeRC, pp. 189–202.

Carapella, E.E., Hyer, M.W., Griffin, O.H., Maahs, H.G., 1994. Micromechanics of crenulated fibers. Journal of Composite Materials 28 (14), 1322–1346.

Chai, H., 1990. Three-dimensional fracture analysis of thin-film debonding. International Journal of Fracture 46, 237–256.

Chang, G.C., Phucharoen, W., Miller, R.A., 1987. Finite element thermal stress solutions for thermal barrier coatings. Surface and Coatings Technology 32, 307–325.

Evans, H.E., 1989. Cracking and spalling of protective oxide layers. Journal of Materials Science and Engineering A 120, 139–146.

Evans, A.G., Hutchinson, J.W., 1984. On the mechanics of delamination and spalling in compressed films. International Journal of Solids and Structures 20 (5), 455–466.

Evans, A.G., Crumley, G.B., Demaray, R.E., 1983. On the mechanical behavior of brittle coatings and layers. Oxidation of Metals 20 (5/6), 193–214.

Kardomateas, G.A., 1989. Transient thermal stresses in cylindrically orthotropic composite tubes. Journal of Applied Mechanics 56, 411–417.

Kardomateas, G.A., 1990. The initial phase of transient thermal stresses due to general boundary thermal loads in orthotropic hollow cylinders. Journal of Applied Mechanics 57, 719–724.

Kardomateas, G.A., Chung, C.B., 1994. Boundary layer transient hygroscopic stresses in orthotropic thick shells under external pressure. Journal of Applied Mechanics 61, 161–168.

Kokini, K., Hornack, T.R., 1988. Transient thermal load effects on coatings bonded to cylindrical substrates and containing circumferential cracks. Journal of Engineering Materials and Technology 110, 35–40.

Mikata, Y., Taya, M., 1985. Stress field in a coated continuous fiber composite subjected to thermo-mechanical loadings. Journal of Composite Materials 19, 554–578.

Neu, R.W., Sehitoglu, H., 1989. Thermomechanical fatigue, oxidation, and creep: part I—damage mechanisms. Met. Trans. A 20A, 1755–1767.

Neu, R.W., Sehitoglu, H., 1989. Thermomechanical fatigue, oxidation, and creep: part II—life prediction. Met. Trans. A 20A, 1769–1783.

Newaz, G.M., Nusier, S.Q., Chaudhury, Z.A., 1998. Damage accumulation mechanisms in thermal barrier coatings. ASME, Journal of Engineering Materials and Technology 120 (2), 149–153.

Nusier, S.Q., Newaz, G.M., 1998. Analysis of interfacial cracks in a TBC/superalloy system under thermal loading. Journal of Engineering Fracture Mechanics 60 (5–6), 577–581.

Nusier, S.Q., Newaz, G.M., 1998. Analysis of interfacial cracks in a TBC/superalloy system under thermo-mechanical loading. Trans. ASME, Journal of Gas Turbines and Power 120 (4), 813–819.

Nusier, S.Q., Newaz, G.M., 1998. Transient residual stresses in thermal barrier coatings: analytical and numerical results. Journal of Applied Mechanics ASME 65 (2), 346–353.

Ryan, R.L., McCafferty, E., 1995. Rupture of an oxide blister. Journal of the Electrochemical Society 142 (8), 2594–2597.

Siegler, D.R., 1993. Adherence behavior of oxide grown in air and synthetic exhaust gas on Fe–Cr–Al alloys containing strong sulfide forming elements Ca, Mg, Y, Ce, La, Ti, and Zr. Oxidation of Metals 40, 555–583.

Suo, Z., 1995. Wrinkles of the oxide scale on an aluminum-containing alloy at high temperature. Journal of the Mechanics and Physics of Solids 43 (6), 829–846.

Takeuchi, Y.R., Kokini, K., 1994. Thermal fracture of multilayer ceramic thermal barrier coatings. Journal of Engineering for Gas Turbines and Power, Trans. ASME 116, 266–271.

Tolpygo, V.K., Grabke, H.J., 1994. Microstructural characterization and adherence of the α-Al_2O_3 Oxide Scale on the Fe–Cr–Al and Fe–Cr–Al–Y alloys. Journal of Oxidation of Metals 41, 343–364.

Williamson, R.L., Rabin, B.H., Drake, J.T., 1993. Finite element analysis of thermal residual stresses at graded ceramic-metal interfaces—part I: model description and geometrical effects. Journal of Applied Physics 74, 1310–1320.

Wittig, L.A., 1993. A micromechanical model of oxidation effects in SiC/Ti metal matrix composites. Master's thesis. Texas A and M University, College Station, Texas.

Wittig, L.A., Allen, D.H., 1994. Modeling the effects of oxidation on damage in SiC/Ti-15-3 metal matrix composites. Journal of Engineering Materials and Technology 116, 421–427.

Wright, K.P., 1996. Private Communication. GE—Evendale, Ohio.

Yin, W., 1985. Axisymmetric buckling and growth of a circular delamination in a compresses laminate. International Journal of Solids and Structures 21 (5), 503–514.